Cellular Multilayer Perceptron for Prediction of Voltages in a Power System

Lisa. L. Grant, *Student Member*, *IEEE* and Ganesh Kumar Venayagamoorthy, *Senior Member*, *IEEE*
Real-Time Power and Intelligent Systems Laboratory
Missouri University of Science & Technology
Rolla, USA
lisagrant@ieee.org, gkumar@ieee.org

***Abstract*—With the increase in renewable energy sources**

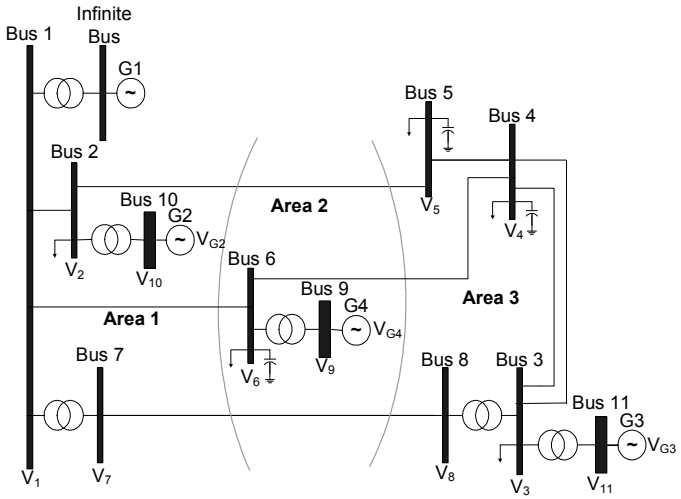

Figure 1.12-bus test power system.

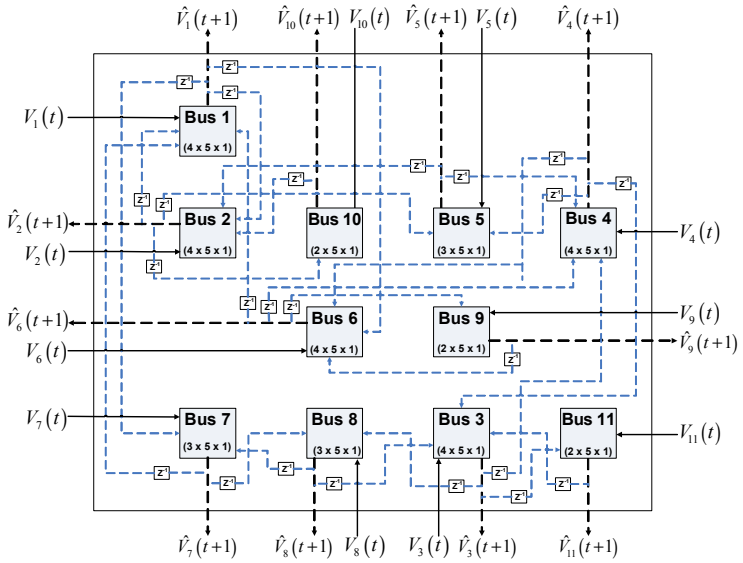

Figure 2. CMLP diagram showing power system equivalent mapping of bus connections.

II. Test Power System

Prediction methods allow for fast local approximation of load flow in power system security assessment. Quick estimation of post-fault bus voltages and line power flows are useful in generating a preliminary contingency screening of a system. It is difficult to test new control methods and algorithms on the real-world power system due to its complexity and cost. To perform this study, the input and desired output data for the neural networks are taken from the power systems modeled in RSCAD software [14].

The voltage profile prediction concept was tested on a small power system. The 12-bus benchmark test power system, shown in Fig. 1, includes six 230-kV buses, two 345-kV buses, and four 22 kV buses [15]. The infinite bus is connected to a 22 kV source. The three area system consists of two hydro-generators (G2 and G4) in areas 1 and 2 respectively, and a thermal generator (G3) in area 3. Parallel transmission lines connect buses 3 and 4. The system is modeled using the detailed synchronous generator models in the RSCAD software with one damper winding on the q axis [14]. The exciter models are IEEE AC1 excitation systems. Parameters of the generator and exciters are given in [15].

III. CMLP Structure and Training

A. CMLP Description

To decrease complexity of training, the neural networks are used to predict the deviations of the bus voltages in per unit. The input and desired output data for the CMLP are taken from the power system simulation. For this study on the 12-bus system, the neural networks are used to predict the voltage deviation at each system bus (ignoring the infinite bus). The bus voltage deviations ($\Delta V_1, \Delta V_2, \ldots, \Delta V_{11}$) are computed from the actual measured voltages at each bus subtracted from the steady state values. The inputs to the CMLP are the voltage deviations monitored at each bus of the power system. The output of the CMLP is the predicted voltage change on each bus at one step ahead in time where each time step is 100 ms. The neural networks should be able to accurately model all of the bus voltages correctly for any power system state. For instance if a disturbance results in an increase of generation, the CMLP should respond to the changes in voltage in the same way as the 12-bus power system modeled in RSCAD would behave.

A Multi-layer Perceptron neural network (MLP) is implemented in each cell of the CMLP. The size of each cell is indicated in CMLP diagram show in Fig. 2. Many voltage stability prediction studies have been carried out using the MLP network [8] [11] [13]. Accuracy and speed of training can be improved by using a CMLP structure due to the small size of the MLP in each individual cell and the ability to train each cell in parallel. Eleven cells are used for this application as applied to the 12-bus power system. Each cell of the CMLP represents one bus in the 12-bus system where the infinite bus (bus 12) is ignored. The connections between the cells represent a direct mapping of the transmission lines that connect the buses in the 12-bus system. Each cell predicts the voltage of bus i that the cell is representing indicated by $\hat{V}_i(t+1)$ at one time step ahead. The dark colored dashed lines in Fig. 2 indicate the predicted outputs of each cell. The inputs to each cell are the actual bus voltage at time t or $V_i(t)$ directly measured from the power system, along with the time-delayed predicted voltage outputs of the buses directly connected to the cell at time t or $\hat{V}_{bus}(t)$. In Fig. 2 the solid lines indicate actual measured bus voltage inputs and the light colored dashed lines indicate the time-delayed bus voltage prediction inputs from the directly connected buses. For example, Cell 1 would be used to predict the voltage on bus 1 or $\hat{V}_1(t+1)$. The inputs to Cell 1 would be the actual measured voltage of bus 1 or $V_1(t)$, and the time-delayed predicted bus voltage outputs of buses 2, 6, and 7 ($\hat{V}_2(t), \hat{V}_6(t), \hat{V}_7(t)$) since those buses are directly connected to Bus 1. The benefit of using one cell to predict the voltage of a single bus using inputs from its nearest

neighboring buses is that for a larger power system the size of each cell's MLP will remain small even though the overall number of cells in the network will increase in direct proportion to the number of buses in the system. Table I contains information on the size of each cell in the CMLP along with the number of weights in each cell. This greatly reduces complexity and computation time when scaling up to perform voltage prediction on larger systems. The training and output of the individual cells can be computed very quickly in parallel with minimal input connections between cells.

TABLE I. SIZE OF EACH CMLP CELL WITH NUMBER OF WEIGHTS

Cell/Bus No.	No. Inputs	No. Hidden	No. Outputs	No. Weights
1	4	5	1	25
2	4	5	1	25
3	4	5	1	25
4	4	5	1	25
5	3	5	1	20
6	4	5	1	25
7	3	5	1	20
8	3	5	1	20
9	2	5	1	15
10	2	5	1	15
11	2	5	1	15
Total	***35***	***55***	***11***	***230***

B. CMLP Training

For MLP weight training, an advanced form of Particle Swarm Optimization (PSO) known as Small Population PSO (SPPSO) is used. Details on the SPPSO algorithm can be found in [16]. PSO was developed by Kennedy and Eberhart in 1995 [17], [18]. In [19], PSO has been show to be a faster training method than backpropagation for neural networks. This swarm intelligence algorithm is based on the behavior of a school of fish or flock of birds. The collective interactions of the individuals in the swarm allow for more optimal solutions to evolve through time. Each member of the swarm, referred to as a particle, randomly searches the environment while updating its position using its own memory and information gathered from the other particles. The particles are given initial random velocities and 'flown' through the problem space. The position that resulted in the particle's best fitness, known as the P_{best} value and the best value of all the P_{best} values defined as the global best position, G_{best}, are stored in memory. The velocities and positions of the particles are updated every iteration until the swarm has converged on the desired solution. The core of the PSO algorithm is the velocity and position update equations given by (1) and (2) respectively. The constants w, c_1, and c_2 are adjusted to determine to what degree the current velocity, personal best, or global best position will affect the particle's next position. The time variable t indicates the current time step in the search.

$$V(t) = w*V(t-1) + c_1*rand_1*\left(P_{best}(t-1) - P(t-1)\right) + c_2*rand_2*\left(G_{best}(t-1) - P(t-1)\right) \quad (1)$$

$$P(t) = P(t-1) + V(t) \quad (2)$$

In SPPSO, a regeneration concept is added that allows the utilization of fewer particles in the swarm, greatly deceasing computation time while maintaining the diversity of the optimization method. For this application, 5 particles were used where standard PSO usually requires 20 to 30 particles. During regeneration 4 of the 5 particles are discarded and replaced by new ones at an interval of every 30 iterations. The G_{best} particle is preserved for each iteration along with the stored P_{best} values. For the CMLP each cell is trained individually so 11 different SPPSO algorithms are used to train the weights of the CMLP, one SPPSO algorithm for each cell. From Table I it can be seen that the SPPSO algorithm for Cell 1 would learn 25 weights and the SPPSO algorithm for Cell 10 would learn only 15 weights. The standard MLP uses a single SPPSO algorithm to train the weights of the entire neural network. For an MLP of size (12x25x11), the single SPPSO algorithm has to learn 575 weights.

The steady state values of the 12-bus system are taken as the bus and generator voltages measured under steady state conditions or with no disturbance after computing the load flow. For training, system disturbances were implemented on the 12-bus system using pseudorandom binary signals (PRBS) fed into the generators' excitation control (buses 9-11) [20]. The PRBS signals excite the natural frequencies of the system. Training in this manner allows the neural network to identify the dynamics of the power system. The disturbance signals are formed by using delayed random noise at different frequencies which are summed to create the PRBS signal. For this application, frequencies of 2, 1, and 0.5 Hz were used.

The generator voltage deviations are taken as the difference between the steady state voltages and the PRBS signal fed into each generator. The bus voltage deviations (ΔV) are the measured voltages at each bus subtracted from the steady state values. For the training set, all three generators PRBS switches were active resulting in disturbances on all of the system generators. For system testing only generators 2 and 3 are excited by the PRBS signals. The bus voltage signals were sampled at 10 Hz for a period of 20 seconds.

C. MLP Neural Network

An MLP is a feed-forward neural network developed by McClellan [21]. This neural network is useful for approximating highly nonlinear functions such as voltage stability. This is done by approximation, association, and pattern matching of the neural network inputs to the outputs of the system by adjusting the weights. This study looks at a standard MLP (size 12x25x11; 575 weights) as a comparison to the CMLP architecture. For the standard MLP pictured in Fig. 3, there are 12 inputs denoted by V, which include the 11 bus voltage deviations (V_1, V_2, ..., V_{11}) and a bias of 1. The outputs of the MLP denoted by $\hat{V}_i(t+1)$ are the predicted bus voltages at the next 100 ms time-step. The standard MLP network uses one MLP to predict the voltages of all 11 power system buses. Given the current bus voltages as inputs, the

MLP will predict the voltage of each of the 11 buses at the next time step. The voltages of the infinite bus (bus 12) are not considered for this application.

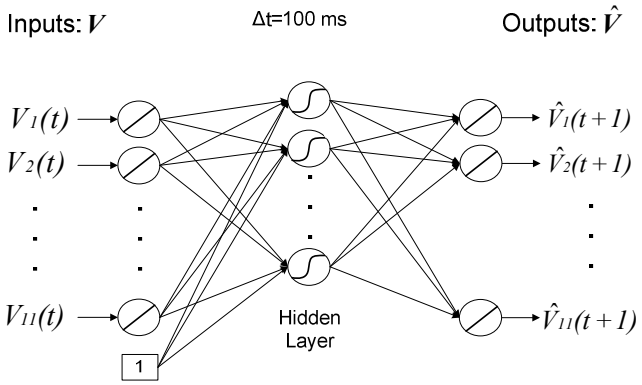

Figure 3. MLP Structure (12x25x11).

IV. RESULTS

Both the CMLP and standard MLP architectures were trained with PRBS signals active on all three generators. The two methods were then tested using data with PRBS signals active on only generators 2 and 3 using the fixed weights found by the SPPSO algorithm in training. The bus voltage signals were sampled at 10 Hz for a period of 20 seconds, which produced 200 samples of data per voltage waveform with a sampling rate of 100 ms. The predicted voltage waveforms of each bus were recorded after testing. Samples of the bus voltage waveform results for the CMLP can be seen in Figs. 4 and 5 where the solid line indicates the actual bus voltage measured from the 12-bus system and the dashed line indicates the bus voltage predicted by the CMLP. Results for the MLP can be seen in Figs. 6 and 7. The results in Figs. 4 and 6 include results for three of the load buses with one load bus from each area (bus 2 – Area 1; bus 6 – Area 2; bus 5 – Area 3). The results in Figs. 5 and 7 include results from the three generator buses (bus 9, bus 10, bus 11). Results were averaged over 20 trials.

From the figures, it is easy to see the quality of the CMLP predictions over the MLP predictions. The CMLP predicted waveforms are very close to the actual waveforms. Even the discrepancies shown in bus 6 and bus 11 CMLP predictions have the correct pattern and are only marginally shifted. The standard MLP falls short in predicting the voltage waveform patterns when compared to the cellular method.

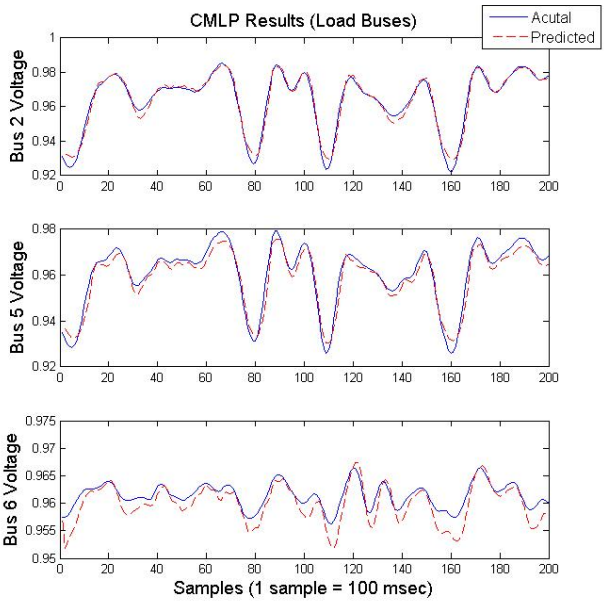

Figure 4. CMLP testing results for load buses.

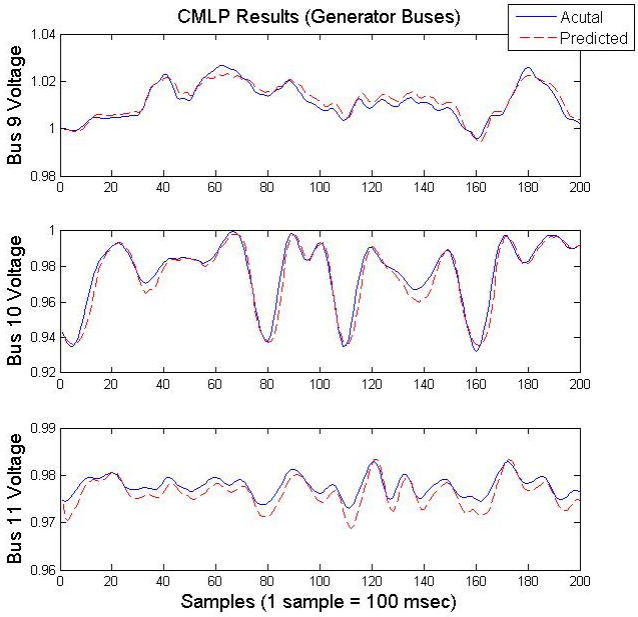

Figure 5. CMLP testing results for generator buses.

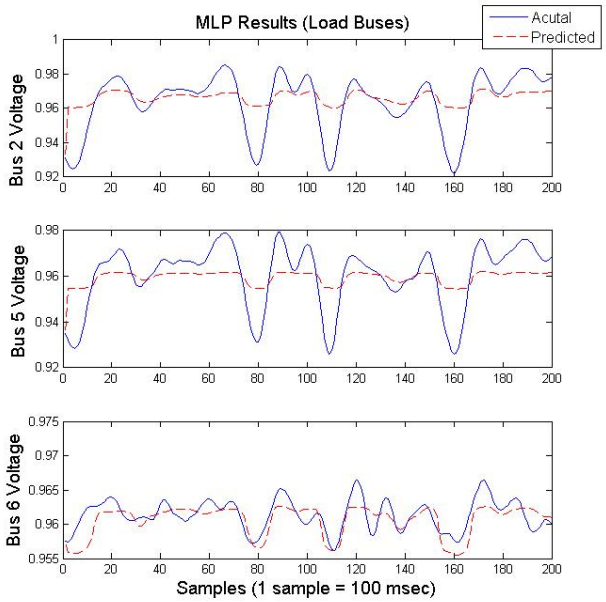

Figure 6. MLP testing results for load buses.

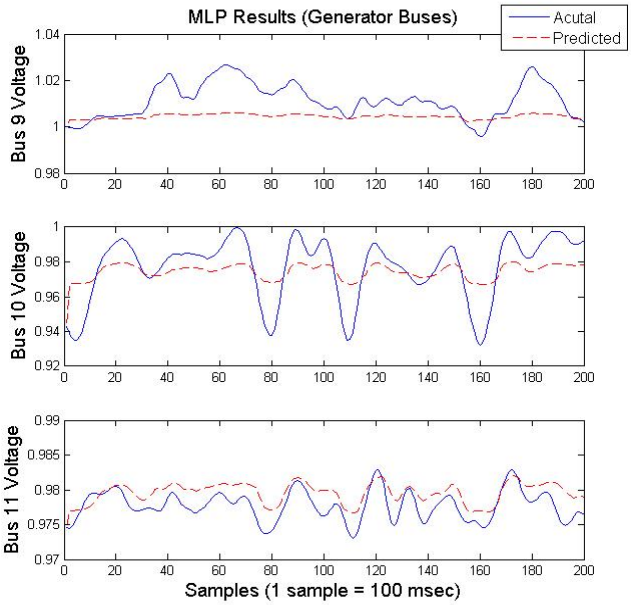

Figure 7. MLP testing results for generator buses.

The fitness of the predicted voltage outputs for both methods was determined by measuring the Mean Square Error (MSE) of the prediction for each bus relative to the actual measured voltage on each bus. Figs. 8 and 9 contain the MSE for each bus of the MLP and CMLP methods for training and testing, respectively. The charts also show the superiority of the CMLP method with all buses MSE being below the MLP MSE. In training, the highest CMLP MSE was 0.28 on bus 2 and the highest MLP MSE was 5.9 on bus 10. The lowest training MSE for CMLP was 0.007 on bus 7 and for MLP was 0.977 on bus 7. Therefore, the worst MSE for CMLP training is still better than the best MSE for the MLP method. Similar trends can be seen for the MSE testing data.

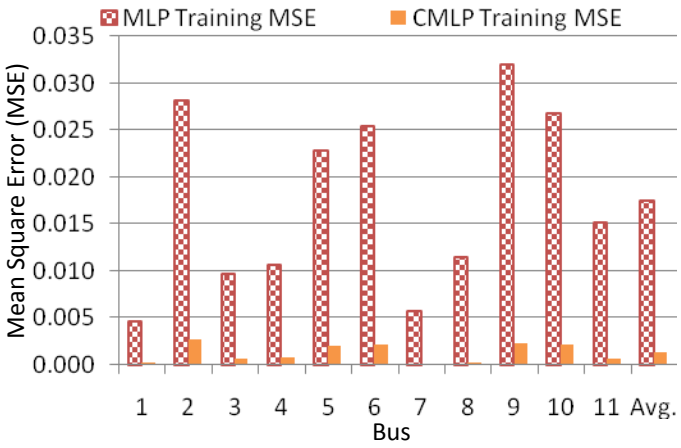

Figure 8. MSE chart for each bus in MLP and CMLP training.

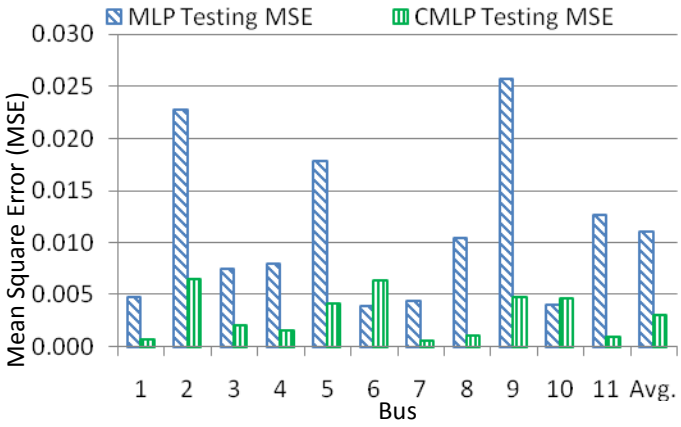

Figure 9. MSE chart for each bus in MLP and CMLP testing.

V. Conclusion

Preliminary studies show that a CMLP is able to accurately predicting the bus voltages of the 12-bus power system and is much more precise than a single standard MLP. By representing a direct mapping of the power system, the CMLP method is easily scalable to larger systems without adding computational complexity and increased runtime. The CMLP produced MSE values 5 times smaller than the MLP using half as many neural network weights. In terms of runtime, the CMLP cells can be processed in parallel since each cell utilizes its own SPPSO training algorithm. Due to the smaller number of weights required for each SPPSO algorithm to learn for the CMLP method being around 20 as compared to the 575 weights that the training algorithm needs to learn for the MLP method, training time is greatly reduced which is desirable for online applications. Future expansion of this work will include fault analysis and testing on larger power systems to prove the scalability of this technique. Other types of neural networks may be explored for use in the cells to try to improve training speed and performance as the complexity of the problem is increased with larger scale power systems.

REFERENCES

[1] C. Taylor, *Power System Voltage Stability*, McGraw Hill, 1994.

[2] P. A. Ruiz, P. W. Sauer, "Voltage and reactive power estimation for contingency analysis using sensitivities," *IEEE Trans. on Power Systems,* vol. 22, no. 2, May 2007, pp. 639-647.

[3] I. Pavic, Z. Hebel, M. Delimar, "Power system equivalent on an artificial neural network" *23rd Intl' Information Technology Interfaces ITI 2001,* Croatia, June 19-22, 2001.

[4] B. Pal, B. Chaudhuri, *Robust Control in Power Systems*, Springer, 2005, pp. 39-178.

[5] S. Sharif, J. Taylor, E. Hill, "On-line optimal power flow by energy loss minimization," *Proc. 35th IEEE Conf. on Decision and Control,* Japan, December 1996.

[6] I. Hiskens, "Power system modeling for inverse problems," *IEEE Trans. on Circuits and Systems*, vol. 51, no. 3, March 2004, pp. 539-551.

[7] G. Chicco, R. Napoli, F. Piglione, "Neural networks for fast voltage prediction in power systems," *IEEE Porto Power Tech Conference*, Portugal, September 2001.

[8] C. A. Belhadj, H. Al-Duwaish, M. H. Shwehdi, A. S. Farag, "Voltage stability estimation and prediction using neural network," *Proc. IEEE Intl' Conference on Power System Technology*, Vol. 2, August 1998, pp. 1464-1467.

[9] C. S. Chang, "Fast power system voltage prediction using knowledge-based approach and on-line box data creation," *Proc. IEEE Generation, Transmission, and Distribution,* vol. 136, no. 2, March 1989, pp. 87-89.

[10] K. C. Hui, M. J. Short, "Voltage security monitoring, prediction and control by neural networks," *IEEE Intl' Conference on Advances in Power System Control, Operation and Management,* November 1991, pp. 889-894.

[11] J. A. Momoh, L. G. Dias, R. Adaa, "Investigation of artificial neural networks for voltage stability assessment," *Proc. Intl' Conference on Intelligent Systems Applications to Power Systems,* February 1996, pp. 410-415.

[12] H. Mori, Y. Komatsu, "A hybrid method of optimal data mining and artificial neural network for voltage stability assessment," *IEEE Russia Power Technology*, June 2005, pp. 1-7.

[13] S. Sahari, A. F. Abidin, T. K. Abdul Rahman, "Development of artificial neural network for voltage stability monitoring," *Proc. National Power and Energy Conference*, Malaysia, 2003, pp. 37-41.

[14] "RSCAD User's Guide, Version 1.204" RTDS Technologies, Inc., Winnipeg, MB, Canada. [Online]. Available www.rtds.org.

[15] S. Jiang, U. D. Nakkage, A. M. Gole, "A platform for validation of FACTS models," *IEEE Trans. on Power Delivery*, vol. 21, no. 1, January 2006, pp. 484-491.

[16] T. K. Das, G. K. Venayagamoorthy, U. O. Aliyu, "Bio-inspired algorithms for the design of multiple optimal power system stabilizers: SPPSO and BFA," *IEEE Trans. on Industry Applications,* vol. 44, no. 5, Oct. 2008, pp. 1445-1457.

[17] J. Kennedy, R. Eberhart, Y. Shi, *Swarm Intelligence,* Morgan Kauffman Publishers, 2001.

[18] J. Kennedy, R. Eberhart, "Particle swarm optimization," *Proc. IEEE Intl' Conference on Neural Networks*, vol. 4, December 1995, pp. 1942-1948.

[19] V. G. Gudise, G. K. Venayagamoorthy, "Comparison of particle swarm optimization and backpropogation as training algorithms for neural networks," *IEEE Swarm Intelligence Symposium*, April 2003, pp. 110-117.

[20] J. Park, G. K. Venayagamoorthy, R. Harley, "MLP/RBF neural-networks-based online model identification of synchronous generator," *IEEE Trans. on Industrial Electronics,* vol. 52, no. 6, December 2005, pp. 1685-1695.

[21] K. C. Hui, M. J. Short, "A neural networks approach to voltage security monitoring and control," *Proc. First Intl' Forum on Applications of Neural Networks to Power Systems,* July 1991, pp. 89-93.